AIAA JOURNAL
Vol. 33, No. 12, December 1995

Experimental Study of Saddle Point of Attachment in Laminar Juncture Flow

Michael D. Coon* and Murray Tobak†
NASA Ames Research Center, Moffett Field, California 94035

An experimental study of laminar horseshoe vortex flows upstream of a cylinder/flat plate juncture has been conducted to verify the existence of saddle-point-of-attachment topologies. In the classical depiction of this flowfield, a saddle point of separation exists on the flat plate upstream of the cylinder, and the boundary layer separates from the surface. Recent computations have indicated that the topology may actually involve a saddle point of attachment on the surface and additional singular points in the flow. Laser light sheet flow visualizations have been performed on the symmetry plane and crossflow planes to identify the saddle-point-of-attachment flowfields. The visualizations reveal that saddle-point-of-attachment topologies occur over a range of Reynolds number in both single and multiple vortex regimes. An analysis of the flow topologies is presented that describes the existence and evolution of the singular points in the flowfield.

Nomenclature

D	= cylinder diameter
h	= cylinder height
N	= node
N'	= half-node
Re_D	= Reynolds number, UD/ν
S	= saddle point
S'	= half-saddle point
U	= freestream velocity
u, v, w	= velocity components in x, y, z direction, respectively
x, y, z	= coordinate system; see Fig. 1
δ^*	= boundary-layer displacement thickness
ν	= fluid viscosity
$\omega_1, \omega_2, \omega_3$	= vorticity components in x, y, z direction, respectively

Subscripts

A	= attachment
S	= separation
x	= partial derivative with respect to x, $\partial/\partial x$
y	= partial derivative with respect to y, $\partial/\partial y$
z	= partial derivative with respect to z, $\partial/\partial z$

Introduction

THE interaction of a boundary layer with a bluff body has been studied in great detail both experimentally and numerically. This interaction is classically represented by the separation of the boundary layer and the formation of a vortex or system of vortices that are swept downstream around the body forming a horseshoe structure, as illustrated in Fig. 1. Recent computational findings[1,2] have revealed alternative flowfield configurations involving a saddle point of attachment rather than one of separation in the skin-friction-line pattern on the surface upstream of the body. In Fig. 2 the symmetry plane streamlines are illustrated for both the classic saddle point of separation and the saddle point of attachment computed in Refs. 1 and 2. The presence of a saddle point of attachment has broad implications in the fundamental understanding of the juncture flow interaction.

A great deal of experimental effort has been devoted to the juncture flow problem. Because of the practical applications of this geometry in the design of wing–body junctions on aircraft and other vehicles, much of the experimental work has involved turbulent boundary layers and high Reynolds numbers.[3–7] However, some notable work has been done in low Reynolds number flows and laminar boundary layers. Schwind[8] studied the interaction of laminar boundary layers with sharp wedges and documented a progression from a single steady vortex to multiple unsteady vortices as the Reynolds number increased. Baker[9,10] investigated the laminar horseshoe vortex around a circular cylinder in great detail and proposed mechanisms for the topological changes with increasing Reynolds number. Thomas[11] examined a range of Reynolds numbers but concentrated on unsteady effects of multiple vortex systems. The possible existence of saddle-point-of-attachment flows may have been overlooked in favor of the saddle-point-of-separation flows that were reported in all of these studies. Only one study,[12] pointed out by Visbal, illustrates what is apparently a saddle-point-of-attachment flowfield.

The juncture flow geometry has also been studied extensively in computations.[13–16] Hung et al.[2] point out that a number of these cases, notably Kaul et al.[13] and Rogers et al.,[14] contain results that may represent saddle-point-of-attachment flowfields. Recent calculations of turbulent flows[17,18] and hypersonic flows[19] have also revealed saddle-point-of-attachment topologies. In addition, computational results have also shown the saddle point of attachment to be important in other geometries, such as the prolate spheroid.[20]

The topological rules[21–23] that are applicable to the vector fields defined by surface skin friction lines and streamlines in flow planes are useful in examining the juncture flow problem and interpreting experimental and numerical results. These rules may be used to determine the physical possibility of various arrangements of singular

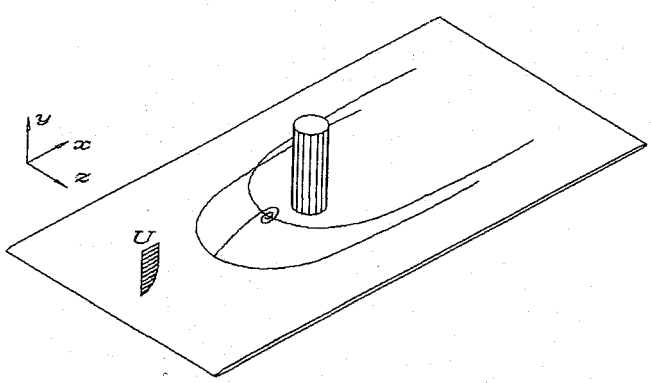

Fig. 1 Model geometry.

Presented as Paper 95-0785 at the AIAA 33rd Aerospace Sciences Meeting, Reno, NV, Jan. 9–12, 1995; received Feb. 11, 1995; revision received June 19, 1995; accepted for publication June 28, 1995. This paper is declared a work of the U.S. Government and is not subject to copyright protection in the United States.

*NRC Associate, MS 260-1. Member AIAA.
†Senior Staff Scientist, MS 260-1. Associate Fellow AIAA.

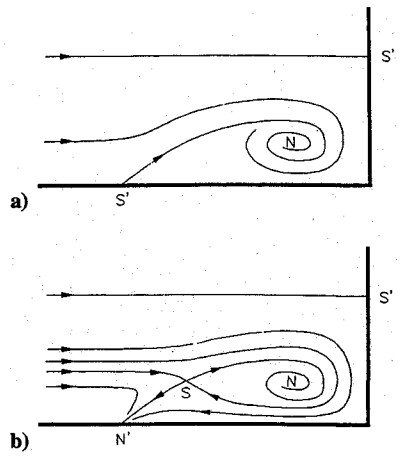

Fig. 2 Symmetry plane schematics: a) saddle point of separation in skin-friction-line pattern and b) saddle point of attachment in skin-friction-line pattern.

points in the flow. Davey[24] and Chapman[25] consider the saddle point of attachment explicitly, but Davey does so in the context of a specific body shape, and Chapman comments on the possibility of its existence but does not consider it further.

In a study of the topologies of flows with saddle points of attachment or separation in the surface flow patterns, Dallmann[26] shows that a given surface flow pattern may support more than one external flow topology. The external flow topologies illustrated in Figs. 2a and 2b exemplify such a circumstance in as much as they share the same surface flow. It is impossible to determine from the surface patterns alone whether the saddle point in the pattern is one of separation or attachment. It is important to keep this ambiguity in mind when examining experimental studies that have relied heavily on surface oil-flow patterns for their interpretation of corresponding external flows.

The purpose of the present study was to investigate experimentally the flowfields computed by Visbal[1] and Hung et al.[2] The primary objective was to utilize flow-visualization techniques to document saddle-point-of-attachment flowfields. Particular attention was paid to the near-surface topology of the vortex interaction to resolve an issue that may have been overlooked in previous studies, namely, the ambiguity in the interpretation of external flows on the basis of surface oil-flow patterns alone. Further work was done to study the progression of the juncture flow interaction from single vortex to multiple unsteady vortices over a range of Reynolds numbers.

Experimental Apparatus and Techniques

This study was conducted in a low-speed water channel at NASA Ames Research Center. The water channel consists of a Plexiglas® test section mounted between two reservoirs. A smooth contraction from the upstream reservoir leads to a honeycomb flow straightener and three fine screens mounted at the upstream end of the test section. The downstream end of the test section is blocked by a weir to control the flow. The test section is 40 cm wide by 122 cm long with a water depth of approximately 25 cm depending on the flow rate. The flow rate was controlled by adjusting a valve on the output of the pump that completes the circuit between the downstream and upstream reservoir and was varied to produce free stream velocities of approximately 1.25–12.0 cm/s.

A splitter plate was used to establish a laminar boundary layer. The splitter plate was 76 cm long, spanned the test section, and was mounted 5 cm above the floor of the channel. The plate was constructed of 1.3-cm Plexiglas with leading and trailing edges machined to 1:8 ellipse cross sections.

Dye flow injection was used to examine the boundary-layer growth on the splitter plate and verify the steadiness of the flow. Velocity measurements from the flow visualizations were used to calculate the undisturbed boundary-layer properties. For comparison, Blasius profiles were calculated using Polhausen's method[27] to account for the elliptical leading edge. The results are shown in Table 1. The highest Reynolds number case shows a boundary-layer thickness substantially higher than the Blasius calculation. This thickening may indicate transition, but the dye flow tests did not indicate unsteadiness.

Table 1 Steady flow test conditions

Re_D	Re_x	U, cm/s	h/D	δ^*/D	(δ^*/D) Blasius
270	3200	1.04	4.0	0.266	0.285
410	2500	0.81	1.5	0.140	0.164
1290	7600	2.49	1.5	0.123	0.093

Stainless-steel and aluminum cylinders of diameters from 0.64 to 5 cm and various heights were positioned on the splitter plate 30.5 cm from the leading edge. The cylinder height to diameter ratio h/D varied from 1.5 to 8. The cylinder height was chosen such that the free end was at least 5 cm below the free surface of the water in the channel. The results for the lower h/D configurations are presented here because the size of the interaction scaled with cylinder diameter D. In the range considered, h/D did not appear to be a relevant parameter.

A laser light sheet was used to enable flow visualization. A 5-W argon-ion laser and cylindrical optics were used to produce a light sheet approximately 3 mm thick that could be aligned with any desired plane in the test section. A rotating filter with transparent, partially transmitting, and opaque regions provided a time base for conversion of the streaklines to velocity vectors and biased the streaklines directionally so that the presence of reversed flow regions would be unambiguous. A number of different types of seed particles were tested to visualize the flow illuminated by the light sheet. The best results were obtained using Pliolite particles. These particles measured 53–74 μm in diameter and had a specific gravity of 1.08.

Laser sheet flow visualization was performed on a variety of planes in the flow. Primarily, the light sheet was aligned with the symmetry plane upstream of the cylinder in order to visualize the attachment point topologies. The light sheet was also aligned along radials from the cylinder at various angles from the symmetry plane in order to visualize the interaction on off-centerline planes. Crossflow components were also visualized by orienting the light sheet in planes both parallel to the flat plate and normal to the free stream. Only the symmetry plane flow visualizations are included herein; the radial and crossflow plane flow visualizations have been omitted for brevity.

For each steady flow studied, long-time exposure photographs of the flow visualization were scanned into a personal computer and traced to provide schematics of the flow structure. From the photographs and schematics, the topology of the flow could be studied, and the presence and type of singular points evaluated. The topology of each case will be considered by applying the appropriate summation rule[21–23] to the flowfield in the symmetry plane bounded by the wall and the leading edge of the cylinder:

$$\Sigma_N + \tfrac{1}{2}\Sigma_{N'} - \left(\Sigma_S + \tfrac{1}{2}\Sigma_{S'}\right) = 0 \qquad (1)$$

A VHS video camera was used to record the laser sheet visualizations of the symmetry plane upstream of the cylinder. The visualizations were recorded while the flow rate was slowly varied to document the changes in topology as the Reynolds number changed. This allowed study of the different flow regimes, as well as the transitions between those regimes. The video was also used to examine the mechanisms of the unsteady vortex motion occurring in the higher Reynolds number systems.

Steady Flow Results

Figure 3 illustrates a low Reynolds number case, $Re_D = 270$. The photograph and tracing clearly show that there is a region of reversed flow but no vortex. As predicted by the computational results,[1,2] there is a saddle point of attachment on the surface, which appears as a half-node of attachment in the symmetry plane, seen in both the photograph (Fig. 3a) and the schematic representation (Fig. 3b). The summation rule [Eq. (1)] is satisfied by the half-node of attachment on the wall and half-saddle point of attachment on the

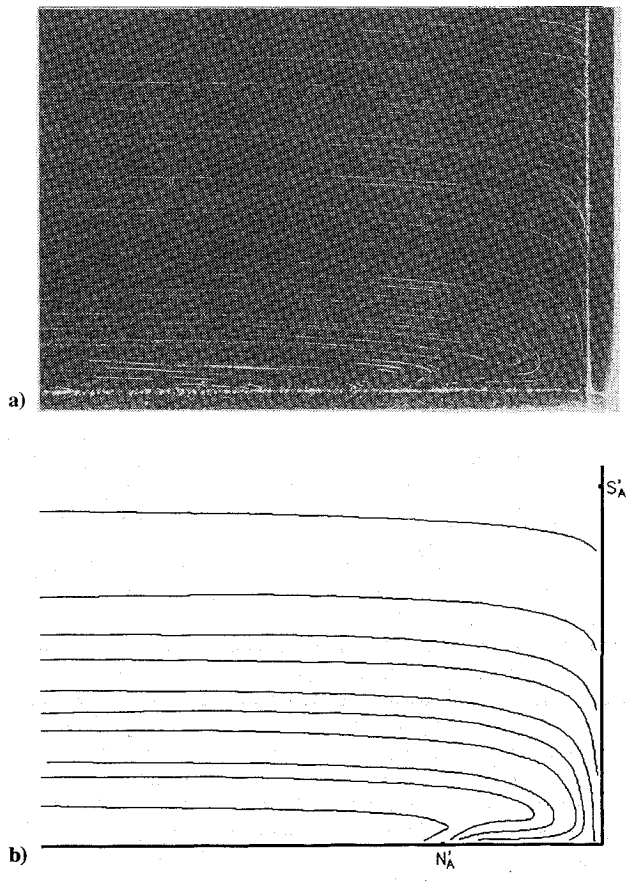

Fig. 3 Symmetry plane, Re_D = 270: a) photograph and b) schematic.

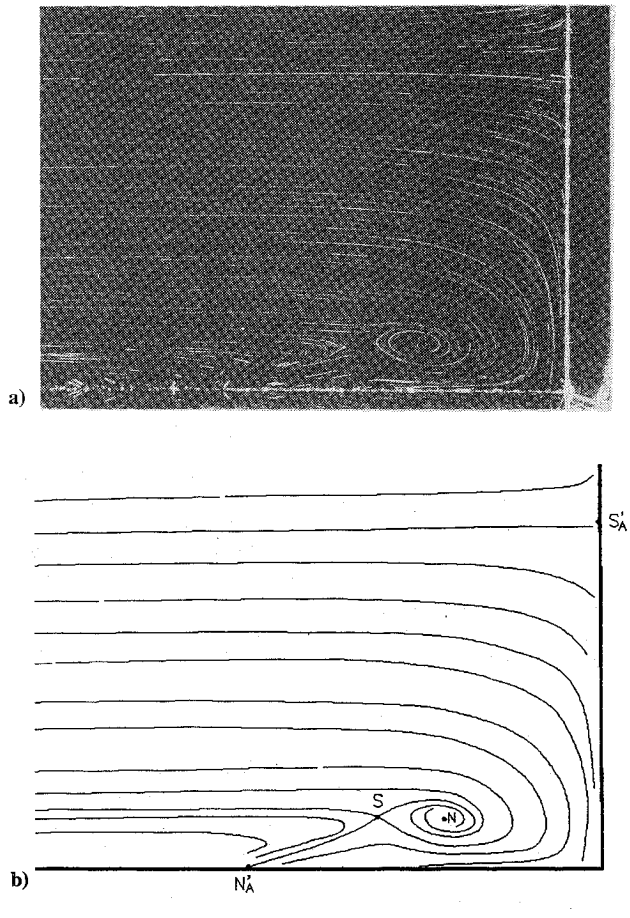

Fig. 4 Symmetry plane, Re_D = 410: a) photograph and b) schematic.

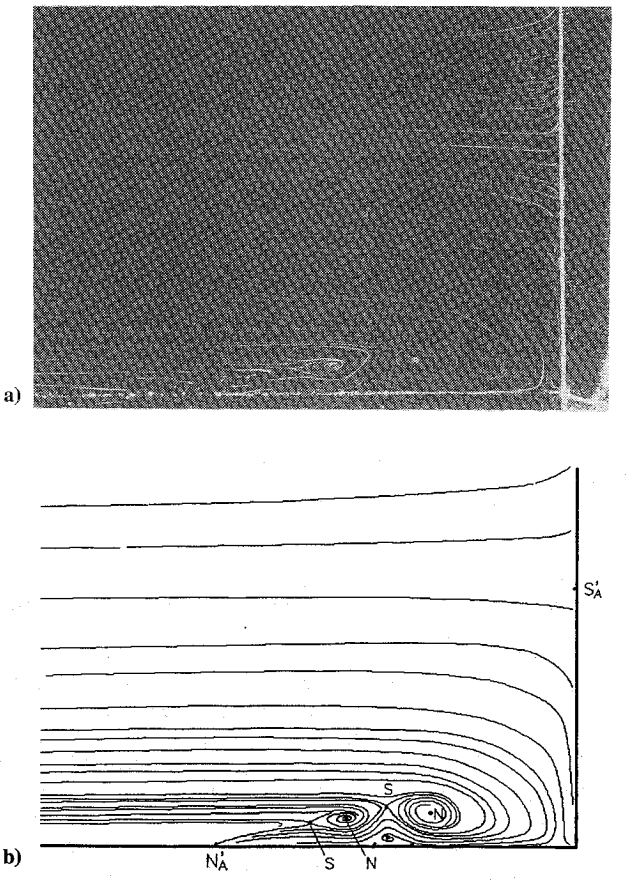

Fig. 5 Symmetry plane, Re_D = 1300: a) photograph and b) schematic.

cylinder leading edge. Note that the resolution of the flow visualization was not adequate to reveal the small separation zone on the cylinder near the juncture, and the details of that interaction have been omitted.

At a slightly higher Reynolds number, $Re_D = 410$, illustrated in Fig. 4, a single vortex is present and there is an associated saddle point in the flow on the symmetry plane. The region of reversed flow and half-node of attachment are clearly visualized. Secondary separations, consisting of a half-saddle point of separation, a focus (node), and a half-saddle point of attachment, may be present but are not visualized. The topological summation rule [Eq. (1)] is satisfied regardless of the presence of secondary separation.

At higher Reynolds number, $Re_D = 1300$, shown in Fig. 5, there are two primary vortices. The half-node of attachment is present, and one secondary vortex is visualized. Consideration of the singularities shows that Eq. (1) is satisfied.

Unsteady Flow Results

The unsteady regimes were studied using the videotape sequences. The onset of unsteadiness occurred at approximately $Re_D = 2500$, varying slightly with h/D. The unsteadiness first appeared as a streamwise translation of the two primary vortices. The vortices move together downstream, toward the cylinder, and then back upstream to their steady flow position.

At a higher Reynolds number, above approximately $Re_D = 3500$, the unsteadiness becomes a cycle of vortex formation, translation, and entrainment. The downstream vortex moves downstream toward the cylinder, contracts, and is swept back upstream and entrained in the upstream vortex. A new vortex is formed at the upstream position during each cycle. This unsteady behavior was documented by Baker[9] and labeled regime 4 in his classification.

The topological summation rule [Eq. (1)] must be satisfied at every instant in the unsteady flows. It is clear from the flow visualizations that the formation and combination of vortices involves node-saddle pairs in each case, so that the summation rule is obeyed.

Theoretical Analysis

The experimental results reported here confirm computational results[1,2] showing that the flow approaching a cylindrical obstacle attached to the wall is able to find an alternative to separation in the classical sense. The alternative is marked by the presence of a saddle point of attachment rather than one of separation in the skin-friction-line pattern at the wall underlying the flow approaching the obstacle. The question needs to be asked: What determines whether the flow separates, originating from a saddle point of separation, or takes the alternative path, originating from a saddle point of attachment?

To address the question, first consider flow conditions that are virtually two dimensional. Let us imagine allowing the diameter of the obstacle to become very large while maintaining constant the properties of the oncoming flow far upstream. Because of the breadth and diminished curvature of the surface facing the oncoming stream, the flow in the vicinity of the symmetry plane will be essentially two dimensional. It is clear that the flow there must separate in the classical sense. This is illustrated in Fig. 6 for the primary state, corresponding to a sufficiently low forward speed of the flow far upstream. Loci of points where $u = 0$ and $v = 0$ cross at a singular point within the flow. The singular point is shown as an inward-spiraling focus (rather than as the center that would be required for a strictly two-dimensional flow). The focus is the origin of the horseshoe vortex that encircles the obstacle and passes downstream. Additional loci are shown in Fig. 6 on which $\nabla^2 v = 0$. We note that for two-dimensional flow,

$$\nabla^2 v = v_{xx} + v_{yy} = \frac{\partial}{\partial x}(v_x - u_y) = \omega_{3x}$$

where ω_3 is the component of vorticity normal to the symmetry plane.

Let us now show that the points on the wall where $\nabla^2 v = \omega_{3x} = 0$ coincide with the points on the wall where the $v = 0$ loci begin. Suppose $v = 0$ on a curve $y = f(x)$ that intersects the $y = 0$ axis at one or more points. The requirements that $v(x, 0) = 0$, $v_y(x, 0) = 0$, and $v = 0$ on $y = f(x)$ can be satisfied in the vicinity of the wall by the expression

$$v = (y^2/2)[y - f(x)]B(x, 0)$$

Then, at the wall,

$$\nabla^2 v = -Bf$$

which will be zero at the points where $f = 0$, i.e., the same points on the $y = 0$ axis that originate the locus at which $v = 0$.

The points at which the loci originate lie on either side of the singular point at the wall originating the separation, where $\omega_3 = 0$. The points in front of the singular point are the result of the growth of wall vorticity to an extremum before the reversal in sign at $\omega_3 = 0$. In the symmetry plane, the singular point is a half-saddle point of separation. Its counterpart in the skin-friction-line pattern is a saddle point of separation.

Now, while maintaining the same flow properties far upstream, consider the effect of a reduction in the diameter of the cylinder of sufficient magnitude to make the flow three dimensional even in the vicinity of the symmetry plane. The transverse velocity w will come into play, where w must be an odd function of the coordinate z normal to the symmetry plane $z = 0$, and is directed away from this plane.

The points at the wall where the loci $v = 0$, $\nabla^2 v = 0$ begin in the symmetry plane continue to coincide (since v_{zz}, the additional contribution to $\nabla^2 v$, is zero at the wall), but now

$$\nabla^2 v = v_{xx} + v_{yy} + v_{zz} = \frac{\partial}{\partial x}(v_x - u_y) - \frac{\partial}{\partial z}(w_y - v_z)$$

$$\nabla^2 v = \omega_{3x} - \omega_{1z}; \qquad \omega_1 = w_y - v_z$$

In the vicinity of the symmetry plane,

$$v = v_0(x, y) + z^2 v_1(x, y)/2$$

$$w = zW(x, y)$$

and so

$$\omega_{1z} = w_{yz} - v_{zz} = W_y - v_1$$

Then, at the wall in the symmetry plane,

$$\nabla^2 v = \omega_{3x}(x, 0) - W_y(x, 0)$$

We see in Fig. 7 that the addition of the positive transverse velocity contribution W_y brings the points where $\nabla^2 v = 0$ at the wall closer together. Following suit, the coincident points where the $v = 0$ loci begin move toward the point on the wall where $\omega_3 = 0$ originates the half-saddle point of separation. The singular point in the flow, where the loci $v = 0$ and $u = 0$ cross, similarly moves toward the singular point at the wall. With each increase in W_y (corresponding to a reduction in the diameter of the cylinder under the same upstream flow conditions) the singular point in the flow ($u = 0$, $v = 0$) will move closer toward the point on the wall where $\omega_3 = 0$ (Fig. 8).

In the limit, there will be a critical value of W_y for which the nodal singular point ($u = 0$, $v = 0$) has reached the wall and merged with the half-saddle point of separation. In the symmetry plane, the point where $\omega_3 = 0$ at the wall has become a half-node of attachment

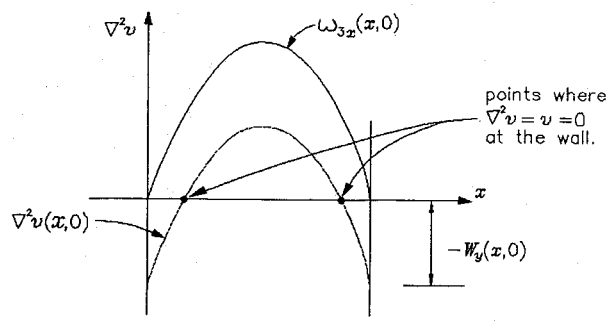

Fig. 7 Effect of transverse velocity contribution W_y on the points where $\nabla^2 v = 0$ at the wall.

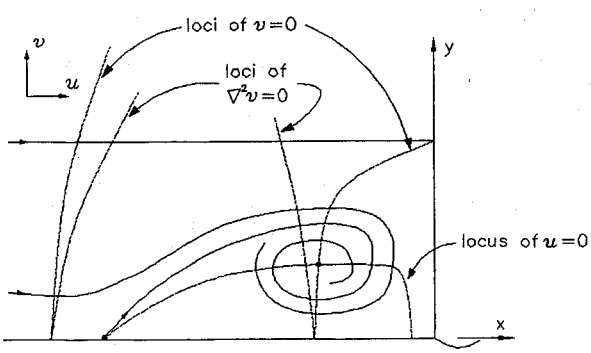

Fig. 6 Separated flow in symmetry plane.

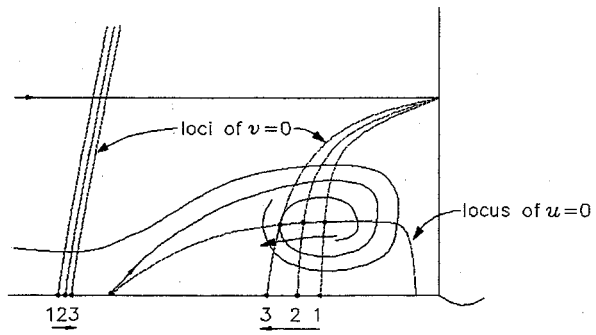

Fig. 8 Effect of successive increase in velocity contribution W_y on location of singular point in flow.

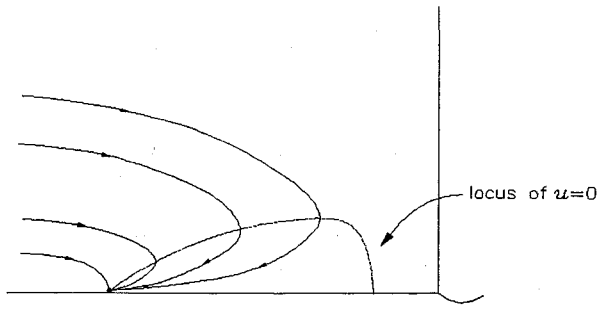

Fig. 9 Merger at the wall of nodular singular point in the symmetry plane and half-saddle of separation at the wall.

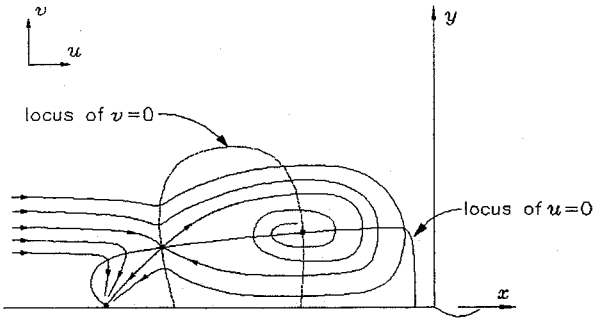

Fig. 10 Configuration of loci after evolution to higher Reynolds number regime.

(Fig. 9). Its counterpart in the skin-friction-line pattern has become a saddle point of attachment. If the cylinder diameter corresponding to the critical value of W_y is now fixed and the Reynolds number is increased by a sufficient increase in the speed of the upstream flow, a new locus of $v = 0$ will form to accommodate an excess in vertical mass flow in the reversed flow region. Intersection of this locus with the existing $u = 0$ locus will lead to the formation of additional singular points in the flow as illustrated in Fig. 10.

Conversely, for a case of increasing cylinder diameter, there will be a critical value of W_y at which separation occurs. In this case, the attachment flow illustrated in Fig. 9 will evolve into a separated flow by the reverse of the process shown in Fig. 8.

We conclude that it is the three dimensionality of the flow approaching the obstacle, characterized by the presence and magnitude of the transverse velocity w, that allows the flow to take an alternative route around the obstacle. Rather than undergoing separation, with the flow rising around a separation stream surface originating at a saddle point of separation, a sufficient quantity of flow may be diverted outward to allow the remainder of the flow to turn downward into a saddle point of attachment.

Conclusions

An experimental investigation of laminar juncture flows has confirmed the presence of a saddle point of attachment upstream of the cylinder juncture. The saddle point of attachment was observed over a range of Reynolds numbers and flow regimes. In no case was a saddle point of separation, the classical configuration, observed.

An analytical explanation of the saddle point of attachment in three-dimensional flows was outlined. The method involves the use of the loci of zeros in the velocity field to examine the topological changes in the flowfield. It provides a theoretical basis for the existence and evolution of flowfields involving singular points.

Whereas the results presented represent a limited range of flow conditions, other studies have indicated that the saddle-point-of-attachment topology exists over a much broader range, including turbulent and high-speed flows. The analysis presented can be extended to these conditions to provide a fundamental understanding of the flowfield evolution.

Acknowledgments

Support for the first author was provided by the National Research Council. The authors wish to thank Ching-Mao Hung and Gary Chapman for constructive discussions during the course of this project.

References

[1]Visbal, M. R., "Structure of Laminar Juncture Flows," *AIAA Journal*, Vol. 29, No. 8, 1991, pp. 1273–1282.

[2]Hung, C. M., Sung, C. H., and Chen, C. L., "Computation of Saddle Point of Attachment," *AIAA Journal*, Vol. 30, No. 6, 1992, pp. 1561–1569.

[3]Fleming, J. L., Simpson, R. L., Cowling, J. E., and Devenport, W. J., "An Experimental Study of a Turbulent Wing-Body Junction and Wake Flow," *Experiments in Fluids*, Vol. 14, No. 5, 1993, pp. 366–378.

[4]Eckerle, W. A., and Langston, L. S., "Horseshoe Vortex Formation Around a Cylinder," *Journal of Turbomachinery*, Vol. 109, April 1987, pp. 278–285.

[5]Pierce, F. J., and Harsh, M. D., "The Mean Flow Structure Around and Within a Turbulent Junction or Horseshoe Vortex—Part II. The Separated and Junction Vortex Flow," *Journal of Fluids Engineering*, Vol. 110, Dec. 1988, pp. 415–423.

[6]Pierce, F. J., and Shin, J., "The Development of a Turbulent Junction Vortex System," *Journal of Fluids Engineering*, Vol. 114, Dec. 1992, pp. 559–565.

[7]Khan, M. J., Trosper, J. R., and Ahmed, A., "On Dynamics of the Juncture Vortex," AIAA Paper 93-3473, Aug. 1993.

[8]Schwind, R. G., "The Three Dimensional Boundary Layer Near a Strut," Massachusetts Inst. of Technology Gas Turbine Lab., Rept. 67, Massachusetts Inst. of Technology, Cambridge, MA, May 1962.

[9]Baker, C. J., "The Laminar Horseshoe Vortex," *Journal of Fluid Mechanics*, Vol. 95, Pt. 2, 1979, pp. 347–367.

[10]Baker, C. J., "The Oscillation of Horseshoe Vortex Systems," *Journal of Fluids Engineering*, Vol. 113, Sept. 1991, pp. 489–495.

[11]Thomas, A. S. W., "The Unsteady Characteristics of Laminar Juncture Flow," *Physics of Fluids*, Vol. 30, No. 2, 1987, pp. 283–285.

[12]Kawahashi, M., and Hosoi, K., "Beam-Sweep Laser Speckle Velocimetry," *Experiments in Fluids*, Vol. 8, Nos. 1, 2, 1989, pp. 109–111.

[13]Kaul, U. K., Kwak, D., and Wagner, C., "A Computational Study of Saddle Point of Separation and Horseshoe Vortex System," AIAA Paper 85-0182, Jan. 1985.

[14]Rogers, S. E., Kwak, D., and Kaul, U. K., "A Numerical Study of Three-Dimensional Incompressible Flow Around Multiple Posts," AIAA Paper 86-0353, Jan. 1986.

[15]Briley, W. R., Buggeln, R. C., and McDonald, H., "Solution of the Three-Dimensional Navier–Stokes Equations for a Steady Laminar Horseshoe Vortex Flow," AIAA Paper 85-1520, July 1985.

[16]Spall, R. E., and Malik, M. R., "The Linear Stability of a Flat Plate Boundary-Layer Approaching a Cylindrical Obstacle," *Journal of Fluids Engineering*, Vol. 114, Sept. 1992, pp. 306–312.

[17]Chen, C. L., and Hung, C. M., "Numerical Study of Juncture Flows," *AIAA Journal*, Vol. 30, No. 7, 1992, pp. 1800–1807.

[18]Rizzetta, D. P., "Numerical Simulation of Turbulent Cylinder Juncture Flowfields," *AIAA Journal*, Vol. 32, No. 6, 1994, pp. 1113–1119.

[19]Dallmann, U., Hilgenstock, A., and Riedelbauch, S., "On the Footprints of Three-Dimensional Separated Vortex Flows Around Blunt Bodies," *Vortex Flow Aerodynamics*, AGARD CP-494, July 1991, pp. 9-1–9-13.

[20]Dallmann, U., Herberg, T., Gebing, H., Su, W. H., and Zhang, H. Q., "Flow Field Diagnostics: Topological Flow Changes and Spatio-Temporal Flow Structure," AIAA Paper 95-0791, Jan. 1995.

[21]Tobak, M., and Peake, D. J., "Topology of Two-Dimensional and Three-Dimensional Separated Flows," AIAA Paper 79-1480, July 1979.

[22]Hunt, J. C. R., Abell, C. J., Peteraka, J. A., and Woo, H., "Kinematical Studies of the Flows Around Free or Surface Mounted Obstacles; Applying Topology to Flow Visualization," *Journal of Fluid Mechanics*, Vol. 86, Pt. 1, 1978, pp. 179–200.

[23]Perry, A. E., and Fairlie, B. D., "Critical Points in Flow Patterns," *Advances in Geophysics*, Vol. 18B, 1974, pp. 299–315.

[24]Davey, A., "Boundary-Layer Flow at a Saddle Point of Attachment," *Journal of Fluid Mechanics*, Vol. 10, Pt. 4, 1961, pp. 593–610.

[25]Chapman, G. T., "Topological Classification of Flow Separation on Three-Dimensional Bodies," AIAA Paper 86-0485, Jan. 1986.

[26]Dallmann, U., "Topological Structures of Three-Dimensional Vortex Flow Separation," AIAA Paper 83-1735, July 1983.

[27]Schlichting, H., *Boundary Layer Theory*, 7th ed., McGraw–Hill, New York, 1955, p. 218.